

Hydro Pac # 793

# Spatial Variability in Hydrologic Properties of a Volcanic Tuff

by J. D. Istok<sup>a</sup>, C. A. Rautman<sup>b</sup>, L. E. Flint<sup>c</sup>, and A. L. Flint<sup>d</sup>

## Abstract

Spatial variability of hydrologic properties was quantified for a nonwelded-to-welded ash flow tuff at Yucca Mountain, Nevada, the potential site of a high-level, nuclear waste repository. Bulk density, porosity, saturated hydraulic conductivity, and sorptivity were measured on core specimens collected from outcrops on a grid that extended vertically through the entire unit thickness and horizontally 1.3 km in the direction of ash transport from the volcanic vent. A strong, geologically determined (deterministic) vertical trend in properties was apparent that correlated with visual trends in degree of welding observed in the outcrop. The trend was accurately described by simple regression models based on stratigraphic elevation (vertical distance from the base of the unit divided by unit thickness). No significant horizontal trends in properties were detected along the length of the transect. The validity of the developed model was tested by comparing model predictions with measured porosity values from additional outcrop sections and boreholes that extended 3000 m north, 1500 m northeast, and 6000 m south of the study area. The model accurately described vertical porosity variations except for locations very close to the source caldera, where the model underpredicted porosity in the upper half of the section. The presence of deterministic geologic trends, such as those demonstrated for an ash flow unit in this study, can simplify the collection of site characterization data and the development of site-scale models.

## Introduction

Site characterization and performance assessment activities are in progress at several existing and potential waste storage and disposal sites in the western United States. The information provided by site characterization typically consists of measurements of hydrologic properties at a limited number of data locations (e.g., core specimens from boreholes). Performance assessment calculations (e.g., water flow or solute transport calculations), however, typically require property values at all locations in a computational grid covering the site. Estimating these values from the available point measurements requires the development of site-scale models to represent the variation in geologic and hydrologic properties of subsurface materials. The development and use of models of this type has been called "data expansion" (Journel and Alabert, 1989); applications to site characterization and performance assessment are discussed in Freeze et al. (1990) and Rautman and Treadway (1991).

Previous studies have demonstrated that soil and rock properties vary vertically and laterally at many sites (Nielsen et al., 1973; Gajem et al., 1981; Healy and Mills, 1991; Rautman and Flint, 1992) and that, in some situations, this variability may be modeled as a stochastic process (Russo

and Bresler, 1981). Sample variograms are convenient tools for quantifying the spatial variability displayed by a regionalized variable and form the basis for a number of estimation and simulation methods. Examples of the use of geostatistical methods to develop site-scale models of hydrologic properties of soils are in Guma (1978), Burgess et al. (1981), and Viera et al. (1981). Geostatistical methods have also been used to quantify the hydrologic properties of rocks, e.g. fracture orientation and size (Smith, 1981; Young, 1987), hydraulic conductivity and unit thickness (Aboufirassi and Marino, 1984), and geochemical composition (Aitchison, 1984).

Only limited information is available about the spatial variability of hydrologic properties of volcanic rocks, although these rocks constitute the principal hydrogeologic units at Yucca Mountain, Nevada, a potential repository for high-level nuclear waste. The potential repository horizon is in the unsaturated zone and water flow through these materials is the subject of ongoing site characterization and performance assessment activities. Recent field investigations have identified the presence of deterministic trends in hydrologic properties within individual ash flow units (Rautman, 1991; Rautman et al., 1993) and that these trends may have a pronounced effect on the unsaturated flow system controlling water flow through the potential repository horizon (Rautman and Flint, 1992). Vertically, hydrologic properties in volcanic rocks may display deterministic trends related to degree of welding within individual cooling units; laterally, hydrologic properties may display deterministic trends related to distance from the source caldera; however, insufficient data are currently available to quantify these trends.

The presence of deterministic (geologically controlled) vertical trends in degree of welding within individual cooling

<sup>a</sup>Department of Civil Engineering, Oregon State University, Corvallis, Oregon 97331.

<sup>b</sup>Geoscience Assessment and Validation Department, Sandia National Laboratories, Albuquerque, New Mexico 87185.

<sup>c</sup>Raytheon Services Nevada, Hydrologic Research Facility, P.O. Box 327, Mercury, Nevada 89023.

<sup>d</sup>U.S. Geological Survey, Hydrologic Research Facility, P.O. Box 327, Mercury, Nevada 89023.

Received July 1993, revised December 1993, accepted March 1994.

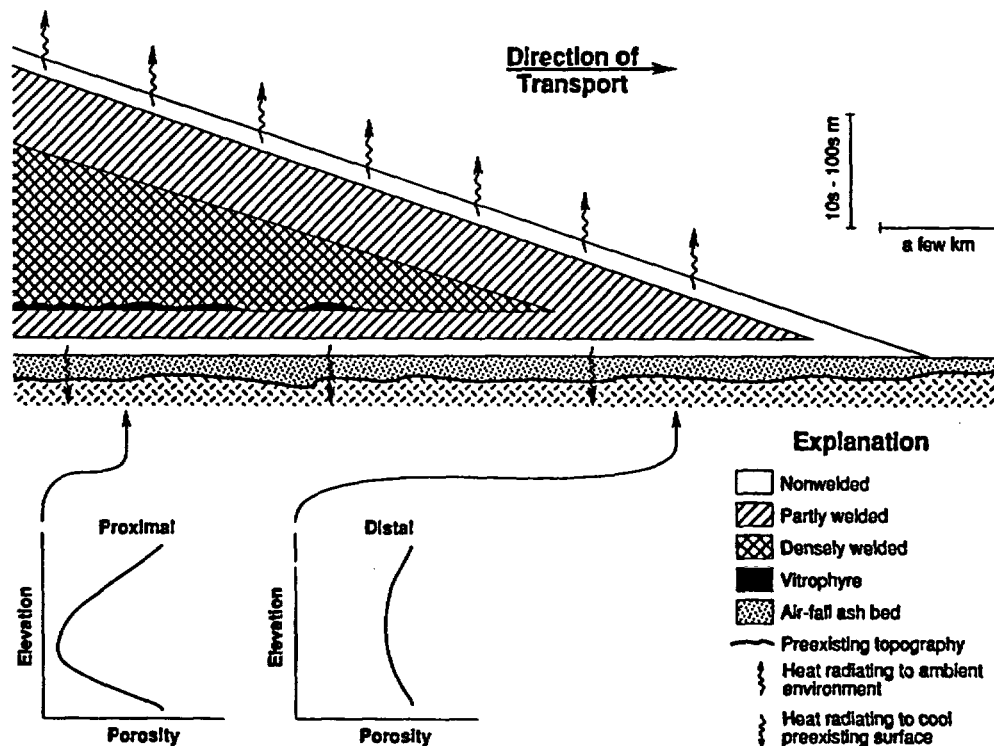


Fig. 1. Conceptual model of cooling unit showing zonation and vertical porosity distribution.

units in tuff deposits is well-known (e.g., Ross and Smith, 1961; Sparks and Wright, 1979). Figure 1 presents a simplified conceptual model of an individual ash flow unit. An ash flow unit is typically underlain by a topography blanketing, Plinian air-fall ash bed (Sheridan, 1979); the thickness of the ash flow unit generally decreases with increasing distance from the source caldera. As the ash cools, zonal features are formed. In the interior of the ash flow unit, high temperatures are maintained for longer periods of time than in the overlying and underlying layers. Heat loss to the preexisting topographic surface is initially rapid, but quickly slows as the temperature of the preexisting surface increases. Heat loss from the upper surface of the ash flow generally continues at a more uniform rate due to convective heat transfer from this surface to the atmosphere. Depending on the rate of cooling, the initially glassy material may devitrify in situ to a microcrystalline aggregate of silica polymorphs and alkali feldspar. Plastic deformation of glassy shards and reduction in porosity can occur as layers compact under the weight of overlying materials. Continued exsolution of magmatic gases into pores (Ross and Smith, 1961) may allow the formation of vapor-phase alteration minerals, again typically microscopic intergrowths of silica phases and feldspar. Vapor phase alteration is typically more advanced in the upper portions of ash flow deposits.

The hydrologic properties of the resulting tuff are significantly influenced by the initial thickness and rate of cooling of the ash, and these vary with position within the cooling unit. For example, a high porosity zone is expected at the base of an ash flow sheet, which cools quickly (Figure 1). Porosity is expected to decrease with increasing elevation in the interior (core) of the flow unit where temperatures

remain high long enough for significant plastic deformation (welding) to occur. The minimum value of porosity is expected near the base of the core because overburden pressure is largest there. Above the core, porosity is expected to first decrease gradually with increasing elevation as overburden pressure decreases, and then to decrease rapidly with increasing elevation through the quickly cooled, uppermost portion of the flow. These vertical trends in porosity are expected to be most strongly expressed in the proximal end of the ash flow, nearest to the source caldera, where the unit is thickest and sufficient overburden pressure is available to produce a densely welded core. These trends are expected to be less apparent at the distal end of the flow, farthest from the source caldera where the unit is thinnest, rapid cooling can occur through a major portion of the ash flow, and overburden pressures are small. Although this conceptual model is generally accepted as valid at Yucca Mountain, variations in magma chemistry, initial temperature, or post-depositional alteration history may produce local variations in this expected profile (Rautman and Flint, 1992).

Although the qualitative features of this conceptual model are well-known, only limited quantitative information is currently available on the distribution of hydrologic properties within individual cooling units. If hydrologic properties can be correlated with more easily observable geologic trends (for example, trends in degree of welding which can be determined visually), it may be possible to simplify site-scale models and reduce sampling and testing requirements for site characterization. The objective of this study was to obtain a detailed description of the spatial variability (vertical and horizontal) in hydrologic properties for the nonwelded-to-welded transition shardy base micro-

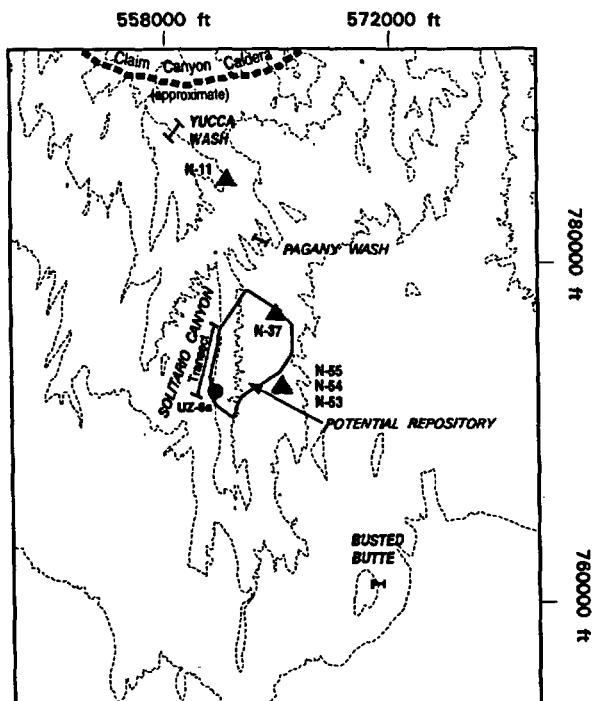


Fig. 2. Location of study area on Nevada Test Site, Nye County, Nevada. Core data were collected from a two-dimensional outcrop sampling transect in Solitario Canyon, vertical outcrop sections at Busted Butte, Pagan Wash, and Yucca Wash, and boreholes N-11, N-37, N-53, N-54, and N-55.

stratigraphic unit of the Tiva Canyon Member of the Paintbrush Tuff at Yucca Mountain. The hydrologic properties of this unit are of importance because under conditions producing fracture flow in the overlying welded tuffs, it could form a capillary barrier or a permeability barrier capable of diverting percolating ground water laterally (Flint et al., 1993). This study presents a quantitative description of the spatial variability of hydrologic properties for the shardy base unit based on an analysis of data for outcrop core specimens collected from an extensive two-dimensional sampling transect. The model developed from the two-dimensional transect is tested by comparison with additional outcrop sampling transects and with core data from recently completed boreholes.

## Methods

### Site Description

Yucca Mountain, located 140 km northwest of Las Vegas, Nevada (Figure 2) consists of alternating welded and nonwelded ash flow and ash fall tuffs that have been tilted toward the east by Basin-and-Range faulting (Carr, 1988). The upper portion of the tuff sequence is well-exposed along the western face of Yucca Mountain in Solitario Canyon.

The principal study area is an extensive outcrop of the shardy base microstratigraphic unit of the Tiva Canyon Member of the Miocene Paintbrush Tuff, located on the western flank of Yucca Mountain (Figure 2). The thickness of the unit ranges from 5 to 15 m along the length of the sampling transect (described below) with an average thickness of 8.3 m. The shardy base microstratigraphic unit consists of three subunits: the upper ash flow, lower ash flow, and pumice bed (Figure 3). The basal pumice bed subunit ranges in thickness from 0.2 to 3 m and is overlain by a nonwelded and poorly sorted lower ash flow subunit, which ranges in thickness from 2 to 8 m. This subunit is overlain by an upper ash flow subunit that changes from nonwelded at the base to densely welded at the gradational upper contact with the overlying columnar microstratigraphic unit. The lower contact of the shardy base is gradational with underlying weathered pumice and ash units; the upper contact of the shardy base is identified in the field by devitrification and vapor-phase alteration, and by the distinctive vertical cooling joints in the overlying columnar microstratigraphic unit.

### Field Sampling

A two-dimensional outcrop sampling transect was established that consisted of 26 vertical sections located between 19 and 200 m apart along a 1.3 km long exposure of the shardy base in Solitario Canyon (Figure 2). The sampling transect extends vertically through the entire

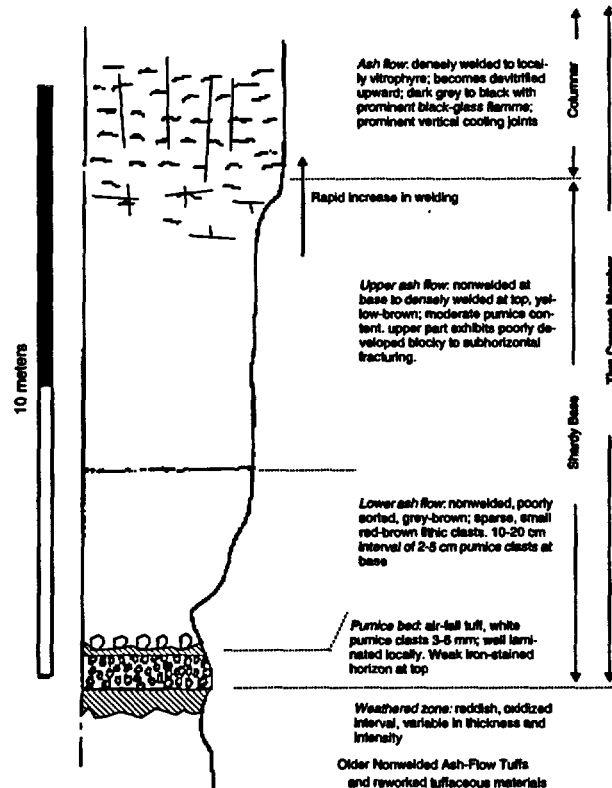


Fig. 3. Schematic stratigraphic profile of part of the Paintbrush nonwelded interval in Solitario Canyon showing position of shardy base transect lithologic interval near drill hole USW UZ-6s.

thickness of the unit and is approximately aligned horizontally with the principal direction of ash transport from the Claim Canyon caldera, the ash source. Ten to 23 core specimens, nominally 2.5 cm in diameter and 4 to 10 cm in length were collected from each vertical section using a portable core drill with a diamond coring bit. Vertical spacing between cores ranged from 0.15 to 2.90 m with an average of 0.76 m. Horizontal distance between vertical sections ranged from 22 to 201 m, with an average of 52.1 m. The horizontal distance ( $x$ ) from the base of each vertical section to an origin established downslope from an existing drill hole (USW UZ-6s) was measured with a steel tape. The vertical distance ( $z$ ) of each core above the base of the basal pumice bed subunit was measured in the field using a Jacob's staff. Stratigraphic elevation,  $E_s = z/D$ , was computed for each core location, where  $D$  is the thickness (measured perpendicular to the bedding plane) of the unit at the vertical section containing the core.

Core specimens were also collected from three additional vertical outcrop sections, located at Yucca Wash, Pagany Wash, and Busted Butte, and from five boreholes: USW UZN-11 (N-11), USW UZN-37 (N-37), USW UZN-53 (N-53), USW UZN-54 (N-54), and USW UZN-55 (N-55) (Figure 2). In an attempt to quantify the magnitude of sampling and testing errors, five closely spaced cores were collected within a total horizontal distance of approximately 1 m at selected locations in the Pagany Wash and Busted Butte outcrop sections.

### Laboratory Analyses

Core specimens were trimmed to a length between 2 and 5 cm using a diamond rock saw. Bulk density ( $\rho_b$ ) and porosity ( $\phi$ ) were determined using Archimedes' principle. Trimmed core specimens were first saturated with carbon dioxide by introducing the gas into an evacuated bell jar containing the cores. Core specimens were then saturated with distilled, deaired water, removed from the bell jar, and dried using a damp towel to remove surface water. Specimens were weighted to determine saturated weight, and weighed while submerged in water to determine saturated volume. The samples were dried in a controlled relative humidity (RH) oven at 60°C and 40% RH and weighed to determine dry weight.

Saturated hydraulic conductivity ( $K$ ) was measured using a constant-head method. Following imbibition measurements, core specimens were encased inside "heat shrink" tubing and connected to a constant-head water supply reservoir. The volume of water flowing through a core specimen for 72 hour period was collected and measured; saturated hydraulic conductivity was computed using Darcy's law. A pressure system (triaxial cell) was used to measure saturated hydraulic conductivity for a few of the more densely welded cores from each vertical section as well as the cores from the Pagany Wash, Yucca Wash, and Busted Butte transects.

Sorptivity (Philip, 1957) was calculated from imbibition data. Imbibition measurements were made using a "tension table" (Klute, 1986). The bottom of the tension table was lined with a cloth towel, a Mariotte reservoir was connected to the inlet port of the tension table and used to

maintain a constant head a few mm above the upper saturated surface of the towel. Core specimens were dried at 60°C and 40% RH, cooled to room temperature, weighed, and then placed on the saturated surface (time,  $t = 0$ ). Periodically, the core specimens were removed, weighed, and returned to the tension table. The equivalent depth of water imbibed into each core as a function of time,  $I(t)$ , was computed from the weight of water imbibed at time  $t$ , the density of water, and the cross-sectional area of the core. Sorptivity ( $S$ ) was calculated for each core by fitting the equation  $I = St^{1/2}$  to the data (Talsma, 1969).

## Results

### Model Development

The data from the two-dimensional outcrop sampling transect in Solitario Canyon was used to develop a quantitative model for the spatial variability of hydrogeologic properties of the shardy base microstratigraphic unit in two directions: vertical (perpendicular to bedding) and horizontal (approximately aligned with the direction of ash transport from the Claim Canyon Caldera). The utility of this model for predicting properties of the shardy base over a large block encompassing the study area was tested by comparing model predictions with measured values of a single hydrogeologic property, porosity, for cores from the Busted Butte, Pagany Wash, and Yucca Wash outcrop sections and from boreholes N-11, N-37, N-53, N-54, and N-55.

### Descriptive Statistics

There were significant differences in properties for the three subunits, reflecting differences in pumice and fine silty ash content, and welding. The basal pumice bed and lower ash-flow subunit are nonwelded. Porosity ( $\phi$ ), hydraulic conductivity ( $K$ ), and sorptivity ( $S$ ) were largest and bulk density ( $\rho_b$ ) was smallest in the basal pumice bed due to the larger percentage of coarse pumice grains in that subunit (Table 1). Porosity,  $\log(K)$ , and  $\log(S)$  were smaller, and  $\rho_b$  was larger in the lower ash-flow subunit than in the pumice bed, reflecting a higher content of ash. Ash contents in the upper and lower ash-flow subunits were similar, but the upper unit had smaller values of  $\phi$ ,  $\log(K)$ , and  $\log(S)$ , and larger values of  $\rho_b$  due to an increase in welding within the upper unit. Properties were generally more uniform (smaller sample standard deviations and coefficients of variation) in the basal pumice bed and lower ash flow subunits than in the upper ash flow subunit (Table 1).

Significant linear correlations existed between the properties. Based on an analysis of scatter plots, linear regression models were fit for  $\log(K)$  and  $\log(S)$  as a function of  $\phi$ :

$$\log(K) = -9.012 + 12.313\phi, r^2 = 0.824 \quad (1a)$$

$$\log(S) = -6.040 + 5.237\phi, r^2 = 0.826 \quad (1b)$$

These regression models are of interest because they provide a means for predicting vertical variation in  $\log(K)$  and  $\log(S)$  based on expected vertical variations in  $\phi$  for the conceptual model in Figure 1, and because  $\phi$  can be measured at more locations (due to lower analysis costs) than  $K$  or  $S$ .

### Deterministic Vertical Trends

The existence of strong vertical trends in properties is apparent in grey-scale plots that show the approximate value and location of measured values for  $\phi$  and  $\log(K)$  (Figure 4). Because of the similarity in trends for  $\phi$  and  $\rho_b$  and for  $\log(K)$  and  $\log(S)$ , only trends in  $\phi$  and  $\log(K)$  will be discussed here. In Figure 4 the contacts between the three subunits are shown by solid lines; the irregular nature of the contacts results in variation in subunit thickness along the length of the transect and in some cases may be due to ash filling of predepositional erosional topography in underlying units. For example, ash filling of a preexisting erosional channel was identified in the field at a distance of 320 m. Porosity and  $\log(K)$  were largest in the basal pumice bed and smallest at the top of the upper ash flow subunit. In the upper ash-flow subunit, and to a lesser extent in the basal pumice bed,  $\phi$  and  $\log(K)$  decreased with increasing elevation above the contact with the underlying subunit. These trends were observed consistently in all vertical sections and were confirmed by field observations of degree of welding (e.g., pumice grain aspect ratios increased during the transition from moderately to densely welded tuff) and by difficulty of drilling, which generally increased with increasing elevation within a section.

A more detailed description of the vertical trends was obtained from an analysis of composite plots prepared by

**Table 1. Descriptive Statistics for Hydrologic Properties for Subunits and Entire Shardy Base Microstratigraphic Unit for Cores from Two-Dimensional Outcrop Sampling Transect in Solitario Canyon**

	$\phi$	$\rho_b$	$\log(K)$	$\log(S)$
<b>Upper ash-flow subunit</b>				
Minimum	0.06	1.30	-8.8	-5.9
Maximum	0.45	2.27	-3.1	-3.4
Mean	0.195	1.89	-6.73	-5.08
Variance	0.010	0.059	1.58	0.263
CV (%)	51	13	19	10
n	130	130	120	122
<b>Lower ash-flow subunit</b>				
Minimum	0.20	1.13	-6.9	-5.2
Maximum	0.55	1.87	-2.2	-2.9
Mean	0.403	1.38	-3.83	-3.83
Variance	0.002	0.012	1.00	0.230
CV (%)	12	8	26	13
n	140	140	133	133
<b>Basal pumice bed subunit</b>				
Minimum	0.34	0.93	-4.5	-4.1
Maximum	0.60	1.54	-1.6	-3.0
Mean	0.520	1.13	2.86	-3.45
Variance	0.004	0.025	0.503	0.070
CV (%)	12	14	25	8
n	36	36	33	35
<b>Entire Shardy Base unit</b>				
Minimum	0.06	0.93	-8.8	-5.9
Maximum	0.60	2.27	-1.6	-2.9
Mean	0.329	1.56	-4.93	-4.31
Variance	0.020	0.117	3.61	0.670
CV (%)	43	22	39	19
n	306	306	286	290

Units for K and S are  $\text{ms}^{-1}$  and  $\text{ms}^{1/2}$ , respectively. CV is coefficient of variation, and n is sample size.

pooling the data for all vertical sections (Figure 5). Porosity decreased with increasing stratigraphic elevation within the basal pumice bed, remained relatively constant within the lower ash-flow subunit, and decreased with increasing stratigraphic elevation within the upper ash-flow subunit [Figure 5(a)]. The rate of decrease in  $\phi$  also decreased with increasing stratigraphic elevation. Contacts between the subunits appeared gradational with respect to  $\phi$ . Trends for  $\log(K)$  and  $\phi$  were similar;  $\log(K)$  decreased with increasing elevation within the basal pumice bed, remained relatively constant within the lower ash-flow subunit, and decreased with increasing stratigraphic elevation in the upper ash-flow subunit [Figure 5(b)]. The nonlinear vertical trends in  $\phi$  and  $\log(K)$  within the upper ash-flow subunit are attributed to the compaction and cooling history of the upper ash-flow subunit. Compaction is at a minimum at the base of the subunit where loss of heat to the underlying, cooler, lower ash flow caused the glass shards to lose their plasticity quickly. Compaction, and eventually welding, of the shards increased upward, in response to the insulating effect of previously deposited materials and the increasing overburden pressure caused by subsequently deposited ash layers. Stratigraphic elevation is useful for displaying these data because it combines data into groups with similar cooling history and overburden pressure.

Several empirical expressions were investigated to describe the observed vertical trends in  $\phi$  and  $\log(K)$ . For  $\phi$ , a three-part regression model was fit using a minimized least-squares procedure

$$\phi = 0.63 - 1.54E_s, \quad 0 \leq E_s < 0.14 \quad \dots (2a)$$

$$\phi = 0.41, \quad 0.14 \leq E_s < 0.35 \quad \dots (2b)$$

$$\phi = 0.11 + 2.21E_s - 4.74E_s^2 + 2.53E_s^3, \quad 0.35 \leq E_s \leq 1.00 \quad \dots (2c)$$

The fitted model is plotted in Figure 5(a); the overall standard error for the fit was 0.04. For  $\log(K)$ , the fitted regression model was

$$\log(K) = -2.39 - 7.09E_s, \quad 0 \leq E_s < 0.14 \quad \dots (3a)$$

$$\log(K) = -3.38, \quad 0.14 \leq E_s < 0.35 \quad \dots (3b)$$

$$\log(K) = 1.74 - 15.71E_s + 0.574E_s^2 + 5.91E_s^3, \quad 0.35 \leq E_s \leq 1.00 \quad \dots (3c)$$

The fitted model is plotted in Figure 5(b); the overall standard error for the fit was 0.78.

Vertical sample variograms were computed by pooling the data for all vertical sections. Sample variograms were computed using regression residuals computed as: residual = observed value - predicted value [using equation (2) or (3)]. Sample variograms for  $\phi$  and  $\log(K)$  regression residuals displayed no substantial spatial correlation and were fit with pure nugget models (Figure 6). The lack of

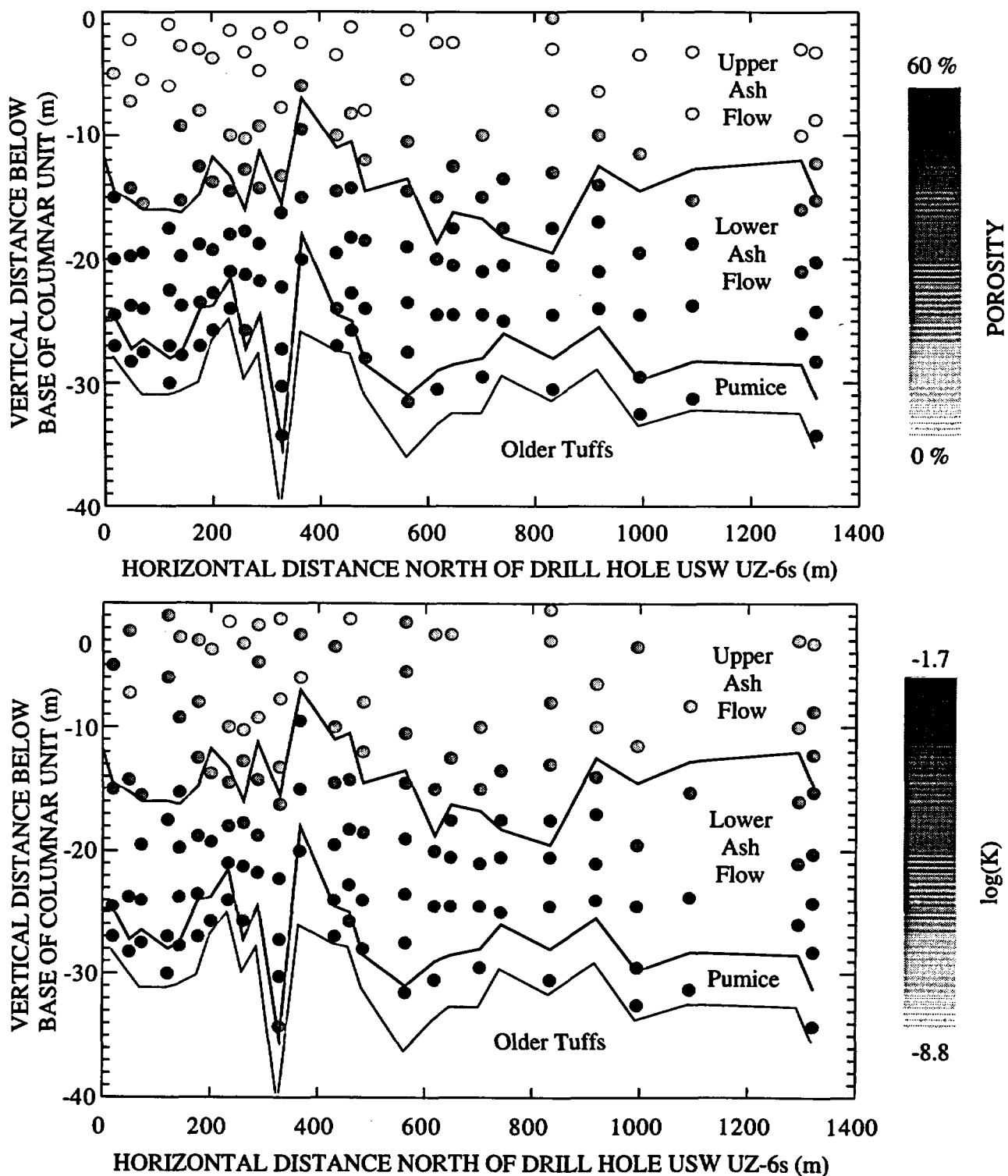


Fig. 4. Horizontal and vertical variation of (a) porosity and (b)  $\log(K)$  for cores from two-dimensional outcrop sampling transect in Solitario Canyon. Measured values are indicated using the grey-scale legend. Solid lines show location of contacts between subunits.

substantial spatial correlation in the vertical direction is further indication that the regression model has accurately described the observed spatial variation in these properties.

#### Analysis of Horizontal Trends

The existence of horizontal trends was investigated by plotting regression residuals vs horizontal distance along the

sampling transect (Figure 7). No systematic trends with horizontal distance for either  $\phi$  or  $\log(K)$  were apparent; an analysis of variance for a fitted linear trend model [with  $\phi$  or  $\log(K)$  as the independent variable and horizontal distance as the dependent variable] confirmed that no significant linear trends existed. Sample variograms for regression residuals for  $\phi$  and  $\log(K)$  were fit with pure nugget models

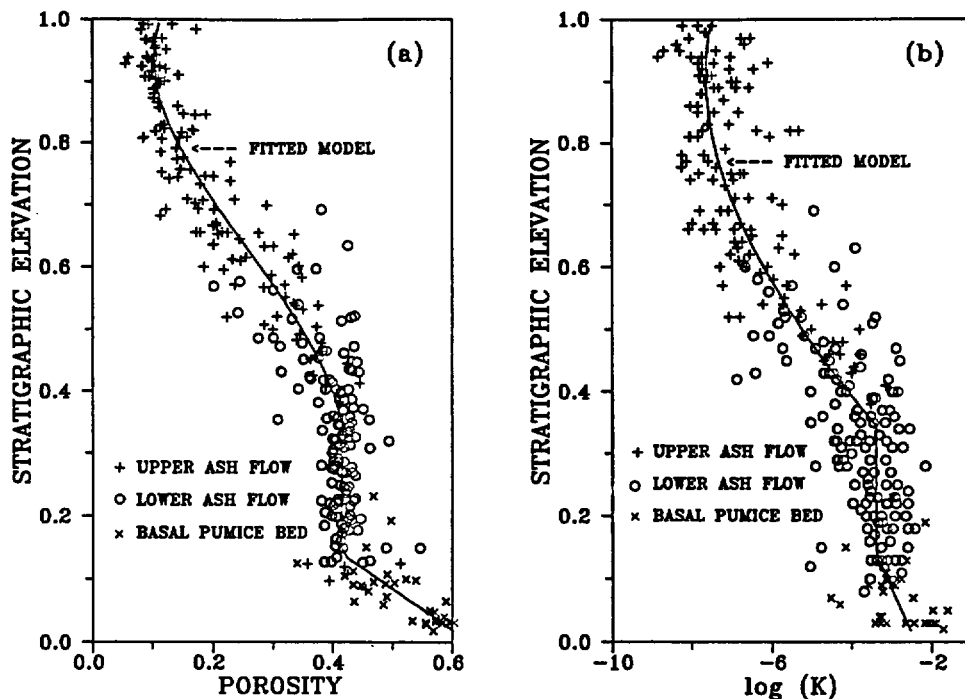


Fig. 5. Fitted regression models (solid lines) for vertical trends in (a) porosity and (b) log(K) for cores from the two-dimensional outcrop sampling transect in Solitario Canyon.

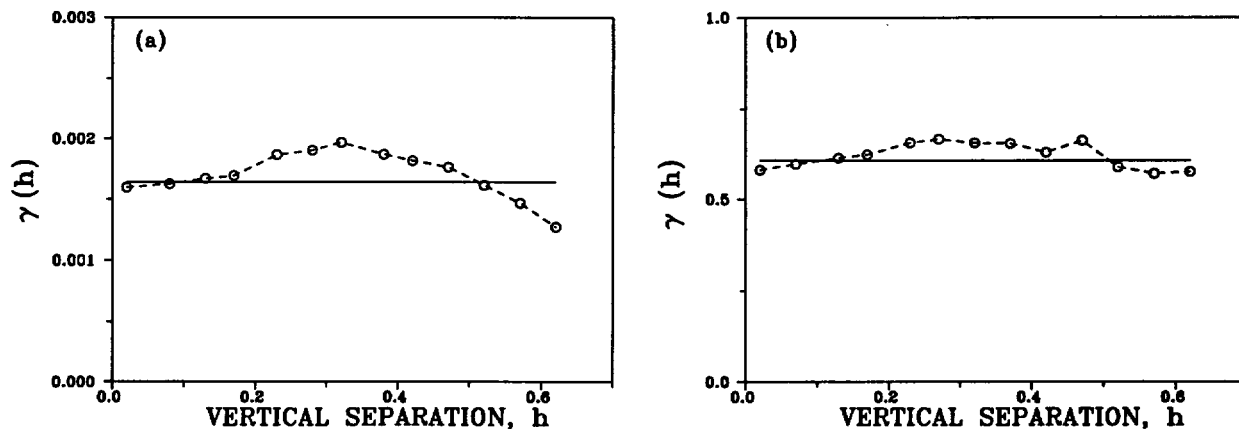


Fig. 6. Vertical sample variograms for regression residuals for (a) porosity and (b) log(K) for pooled data from all vertical sections in the Solitario Canyon outcrop sampling transect. Horizontal line represents variance of regression residuals.

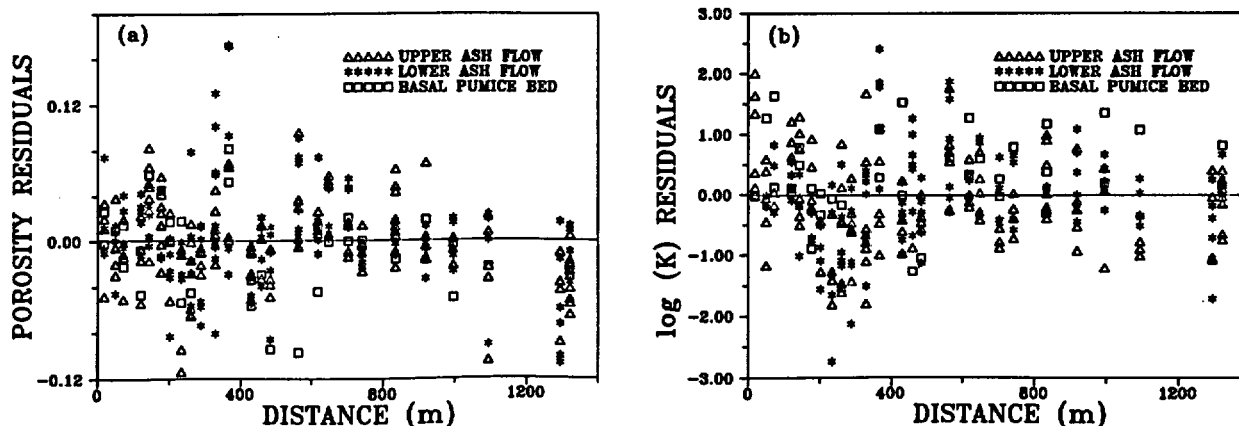


Fig. 7. Regression residuals for (a) porosity and (b) log(K) for pooled data for all vertical sections in the Solitario Canyon outcrop sampling transect.

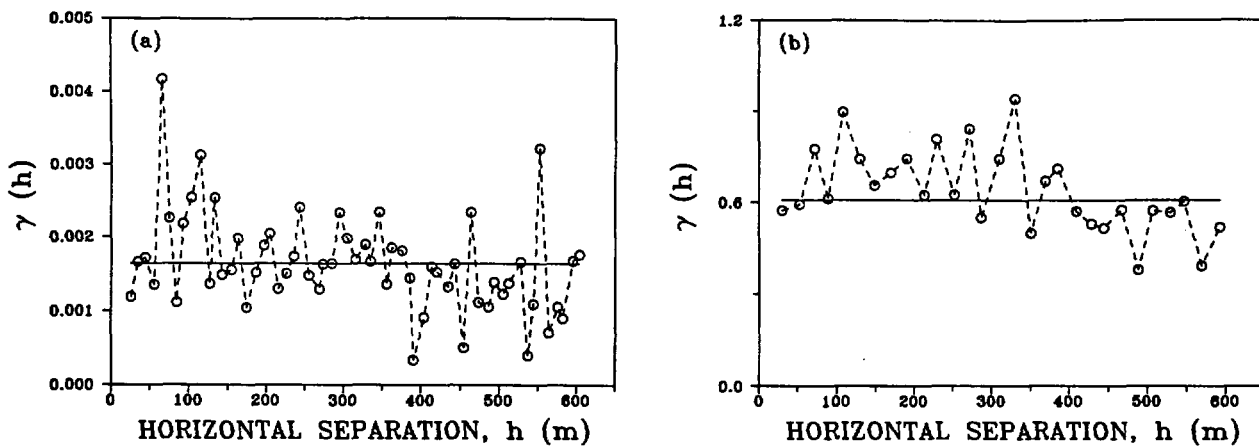


Fig. 8. Horizontal sample variograms for regression residuals for (a) porosity and (b)  $\log(K)$  for pooled data from all vertical sections in the Solitario Canyon outcrop sampling transect. Horizontal line represents variance of regression residuals.

indicating an apparent absence of spatial correlation (Figure 8). The lack of substantial spatial correlation in the horizontal direction suggests that properties can be considered to be essentially constant (except for nonstructured random variations) in this direction.

### Model Validation

Equations (2) and (3) accurately described the observed vertical trends in  $\phi$  and  $\log(K)$  within the shardy base over the entire thickness and length of the Solitario Canyon sampling transect. The utility of equation (2) for predicting  $\phi$  over a larger area encompassing the potential repository was tested by comparing model predictions with measured values of porosity at three additional vertical outcrop sections and five boreholes. The Yucca Wash section was located approximately 2800 m north of the northern edge of the Solitario Canyon transect (Figure 2) and represents a depositional environment much closer to the Claim Canyon Caldera. The Busted Butte section was located approximately 3200 m southwest of the southern edge of the Solitario Canyon transect (Figure 3) and represents a depositional environment further from the caldera. The Pagany Wash section was located approximately 1500 m north and east of the Solitario Canyon transect. The thickness of the shardy base is 14 m at Yucca Wash, 4 m at Busted Butte, and 11 m at Pagany Wash. Four of the boreholes (N-37, N-53, N-54, and N-55) are located from 1000 to 1500 m east, and borehole N-11 is located approximately 2400 m north of the Solitario Canyon transect.

Predicted values of  $\phi$  were obtained for each core in these sections and boreholes using equation (2). Comparisons between measured and predicted values were very good for the Pagany Wash section but were poor for borehole N-11 (Figure 9). Prediction errors (measured - predicted value) for all sections and boreholes are compared in Figure 10. A prediction error of zero indicates a perfect fit; the region within the two vertical dashed lines represents the 95% confidence interval for the model predictions. At Pagany Wash and Busted Butte, prediction errors were small, with a mean value of zero and absolute values generally within two standard errors (shown as vertical dashed lines) of the fitted equations [Figure 10(a)]. For these sec-

tions, prediction errors fluctuated randomly about zero, with no systematic deviation from model predictions. The model predicted more poorly at Yucca Wash, the section closest to the source caldera. There, the model underestimated porosity, especially in the upper half of the section [Figure 10(a)]. The largest prediction errors were several times larger than the average sampling error [shown as a horizontal bar in Figure 10(a)] determined from an analysis of porosity data for the replicate core specimens from the Pagany Wash and Busted Butte outcrop sections, suggesting that prediction errors are not an artifact of sampling and laboratory testing.

The model accurately predicted the vertical distribution of  $\phi$  at borehole N-55, but performed more poorly in predicting  $\phi$  for the other boreholes [Figure 10(b)]. Prediction errors were generally within two standard errors of model prediction for cores from the lower portion of the profile (stratigraphic elevations smaller than 0.4). At higher positions in the section, the model systematically underpredicted  $\phi$ ; approximately one-half of prediction errors exceeded the 95% confidence interval for the model fit. The poorest fit was obtained for borehole N-11, the borehole located closest to the caldera.

The failure of equation (2) in predicting porosity in the upper portion of the section at the northernmost outcrop sections and boreholes may be due to the proximity of these locations to the source caldera and involvement of these regions in the transition from the intracaldera to outflow-sheet environment. Although the location of the exact margin of the Claim Canyon Caldera is uncertain, the Yucca Wash and N-11 sections are within 2 to 3 km of this major structural feature (Byers et al., 1976). Geologically, there are profound differences in the geology of the Tiva Canyon Member in the vicinity of the Yucca Wash transect: the unit is thin and major parts of the welded portion of the unit are missing or of completely different character. There are also qualitative differences in the geology and appearance of the shardy base microstratigraphic unit, although these have not yet been systematically described or evaluated. Hildreth and Mahood (1986) discuss subtle differences within the Bishop Tuff (derived from the Long Valley Caldera near Reno, Nevada) that indicate large-volume ash-flow sheets

Fi  
be  
  
ar  
th  
G  
th  
be  
ex

Fi  
tra  
rep

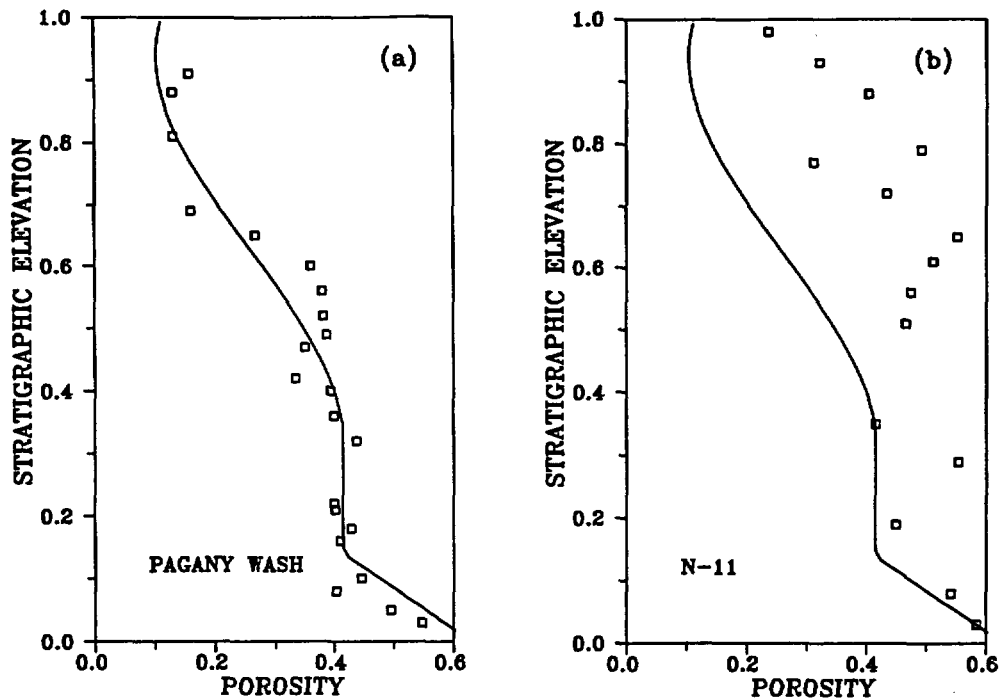


Fig. 9. Comparison of model predictions with measured values of porosity for (a) vertical outcrop section in Pagany Wash and (b) borehole N-11.

are emplaced as numerous individual flows of lobate form that may bypass or overlap one another in complex fashion. Given our preliminary information, it appears reasonable that the northern portion of the Yucca Mountain region has been affected by these types of processes to a much greater extent than the more distal portions of the outflow sheet

sampled by the remaining transects and boreholes.

### Summary

Detailed field sampling and laboratory testing identified the presence of geologically determined vertical trends in hydrologic properties for a nonwelded ash-flow tuff at the

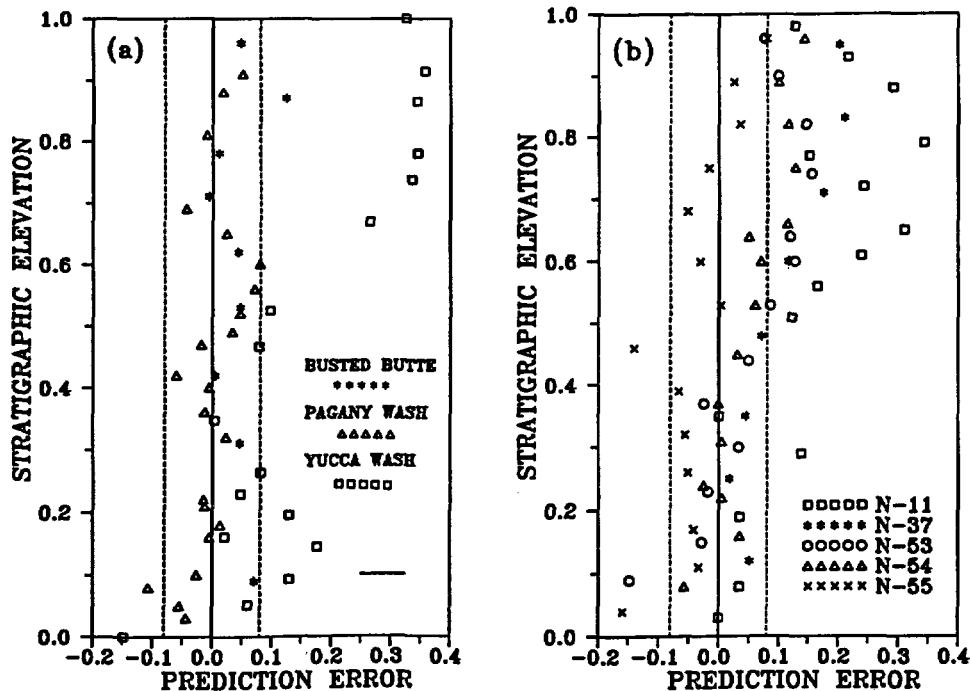


Fig. 10. Validation of vertical trend model developed in Solitario Canyon with measured values of porosity for (a) outcrop sampling transects and (b) boreholes. Dashed vertical lines give approximate 95% confidence levels for fitted model. Horizontal bar in (a) represents magnitude of sampling and measurement errors.

site of a potential high-level nuclear waste repository. The trends were accurately described for a large portion of the study area by simple regression models based on stratigraphic elevation (vertical distance from the base of the unit divided by unit thickness). The validity of the developed model was tested by comparing model predictions with measured porosity values from additional outcrop sections and boreholes. The model accurately described vertical porosity variations in two of the outcrop sections and four of the five boreholes but generally underpredicted porosity for the outcrop section and boreholes located closest to the caldera (the proximal edge of the ash flow).

### Application of Results

Models of hydrogeologic properties are needed for site characterization and performance assessment at many existing and potential waste disposal sites. The presence of geologically determined (deterministic) trends, such as those demonstrated in this study for the shardy base microstratigraphic unit at Yucca Mountain, can simplify the development of these models by providing additional information for use in sampling design, property estimation between boreholes and core samples, and for property simulation. For example, the fitted trends presented here can be used, in conjunction with data from existing borehole and outcrop samples, to obtain preliminary estimates for the shardy base unit over the potential waste repository block. These trends can also be used to simulate geologically plausible sets of rock properties for this unit for use in water-flow calculations. For example, the results indicate that it should be possible to generate porosity and log(K) fields for the potential repository block using equations (2) and (3) (and random error components) with very little computational effort. These fields could then be used as input for Monte Carlo .ype simulation.s of water flow within the shardy base. To the extent that the regression equations quantify actual geologic processes within the cooling ash flow, incorporation of those trends brings a degree of understanding into the modeling process beyond the information contained solely in the tabulated values of hydrogeologic properties.

### Acknowledgments

This work was supported by the U.S. Department of Energy, Yucca Mountain Site Characterization Project Office, under contract DE-AC04-76D00789 and Interagency agreement DE-AI08-78ET44802.

### References

- Aboufirassi, M. and M. A. Marino. 1984. Cokriging of aquifer transmissivities from field measurements of transmissivity and specific capacity. *Mathematical Geology*. v. 16, no. 1, pp. 19-36.
- Aitchison, J. 1984. The statistical analysis of geochemical compositions. *Mathematical Geology*. v. 16, no. 6, pp. 531-564.
- Burgess, T. M., R. Webster, and A. B. McBratney. 1981. Optimal interpolation and isarithmic mapping of soil properties. IV. Sampling strategy. *J. Soil Science*. v. 32, pp. 643-659.
- Byers, F. M., W. J. Carr, R. L. Christianson, P. W. Lipman, P. P. Orkild, and W. D. Quinlivan. 1976. Geologic map of the Timber Mountain Caldera area, Nye County, Nevada. U.S. Geol. Surv. Misc. Inv. Series Map I-891. 1:48,000.
- Carr, W. J. 1988. Volcano-tectonic setting of Yucca Mountain and Crater Flat, southwestern Nevada. U.S. Geol. Survey Bulletin 1790. p. 35.
- Flint, A. L., J. A. Hevesi, and L. E. Flint. 1993. The influence of long-term climate change on net infiltration at Yucca Mountain, Nevada. Proceedings of the Fourth International Conference on High-Level Radioactive Waste Management, Las Vegas, NV.
- Freeze, R. A., J. Massmann, L. Smith, T. Sperling, and B. James. 1990. Hydrogeological decision analysis: I. A framework. *Ground Water*. v. 28, no. 5, pp. 738-766.
- Gajem, Y. M. A. W. Warrick, and D. E. Myers. 1981. Spatial structure of physical properties of a Typic Torrifluent soil. *Soil Society of America Journal*. v. 45, pp. 709-715.
- Guma, G. S. 1978. Spatial variability of in situ available water. Ph.D. dissertation, The Univ. of Arizona, Tucson.
- Healy, R. W. and P. C. Mills. 1991. Variability of an unsaturated sand unit underlying a radioactive-waste trench. *Soil Science Society of America J.* v. 55, no. 4, pp. 899-907.
- Hildreth, W. and G. A. Mahood. 1986. Ring-fracture eruption of the Bishop Tuff. *Geological Society America Bulletin*. v. 97, pp. 396-403.
- Journel, A. G. and F. Alabert. 1989. Non-Gaussian data expansion in the earth sciences. *Terra Nova*. v. 1, pp. 123-129.
- Klute, A. (ed.). 1986. Methods of soil analysis, Part 1, Physical and mineralogical methods. 2nd ed. American Society of Agronomy, Madison, WI.
- Nielsen, D. R., J. W. Biggar, and K. T. Erh. 1973. Spatial variability of field-measured soil-water properties. *Hilgardia*. v. 42, pp. 215-259.
- Philip, J. R. 1957. Theory of infiltration, 1. The infiltration equation and its solution. *Soil Science*. v. 83, pp. 345-357.
- Rautman, C. A. 1991. Estimates of spatial correlation in volcanic tuff Yucca Mountain, Nevada. Sandia National Laboratories, Albuquerque, NM. SAND89-2270.
- Rautman, C. A., J. D. Istok, A. L. Flint, and L. E. Flint. 1993. Influence of deterministic geologic trends on spatial variability of hydrologic properties in volcanic tuff. High-Level Radioactive Waste Management, Proceedings of the Fourth International Conference, Am. Nuc. Soc., LaGrange Park, IL.
- Rautman, C. A. and A. L. Flint. 1992. Deterministic geologic processes and stochastic modeling. Sandia National Laboratories, Albuquerque, NM. SAND91-1925C.
- Rautman, C. A. and A. H. Treadway. 1991. Geologic uncertainty in a regulatory environment: An example from the potential Yucca Mountain nuclear waste repository site. *Environ. Geol. Water Science*. v. 18, no. 3, pp. 171-184.
- Ross, C. S. and R. L. Smith. 1961. Ash-flow tuffs: their origins, geologic relations, and identification. U.S. Geol. Survey, Professional Paper 366.
- Russo, D. and E. Bresler. 1981. Soil hydraulic properties as stochastic processes: I. An analysis of field spatial variability. *Soil Science Society of America J.* v. 45, pp. 682-687.
- Scott, R. B. and J. Bonk. 1984. Preliminary geologic map of Yucca Mountain, Nye County, Nevada with geologic sections. U.S. Geol. Survey Open-File Rept. 84-494.
- Sheridan, M. F. 1979. Emplacement of pyroclastic flows: A review. *Geological Society of America Special Paper* 180. pp. 125-136.
- Smith, L. 1981. Spatial variability of flow parameters in a stratified sand. *Mathematical Geology*. v. 13, no. 1, pp. 1-22.
- Sparks, R. S. J. and J. V. Wright. 1979. Welded air-fall tuffs. *Geological Society America Special Paper* 180. pp. 155-156.
- Talsma, T. 1969. In situ measurement of sorptivity. *Australian J. Soil Research*. v. 7, pp. 269-276.
- Viera, S. R., D. R. Nielsen, and J. W. Biggar. 1981. Spatial variability in field measured infiltration rate. *Soil Science Society of America Journal*. v. 45, pp. 1040-1048.
- Young, D. S. 1987. Indicator kriging for unit vectors: Rock joint orientations. *Mathematical Geology*. v. 19, no. 6, pp. 481-501.

# GROUND WATER



JOURNAL • ASSOC. OF GROUND WATER SCIENTISTS & ENGINEERS • SEPTEMBER—OCTOBER 1994